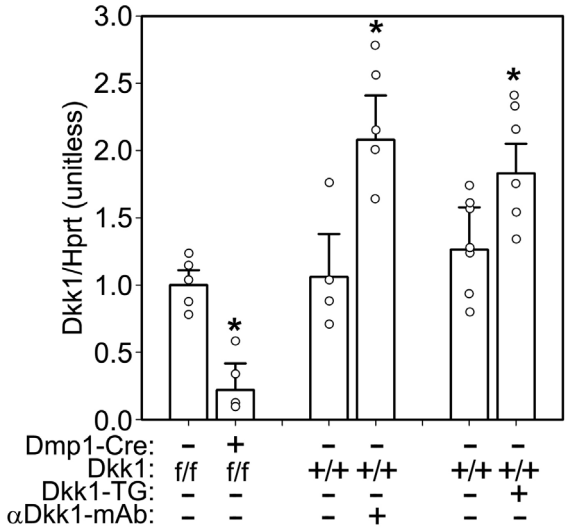

Figure S1: Quantitative PCR of Dkk1 transcripts in the femoral and tibial cortical bone from female mice with conditional (10kbDmp1-Cre-mediated) homozygous inactivation of Dkk1 (left bars), from female wild-type mice treated with αDkk1-mAb (center bars), and from female $^{2.3kb}$Col1a1-Dkk1 mice that overexpress Dkk1 in bone tissue (Dkk1-TG; right bars). *P<0.05 compared to corresponding controls. N=4-7 mice/group. Data were analyzed using 1-way ANOVA, followed by Fisher's protected LSD post hoc tests.

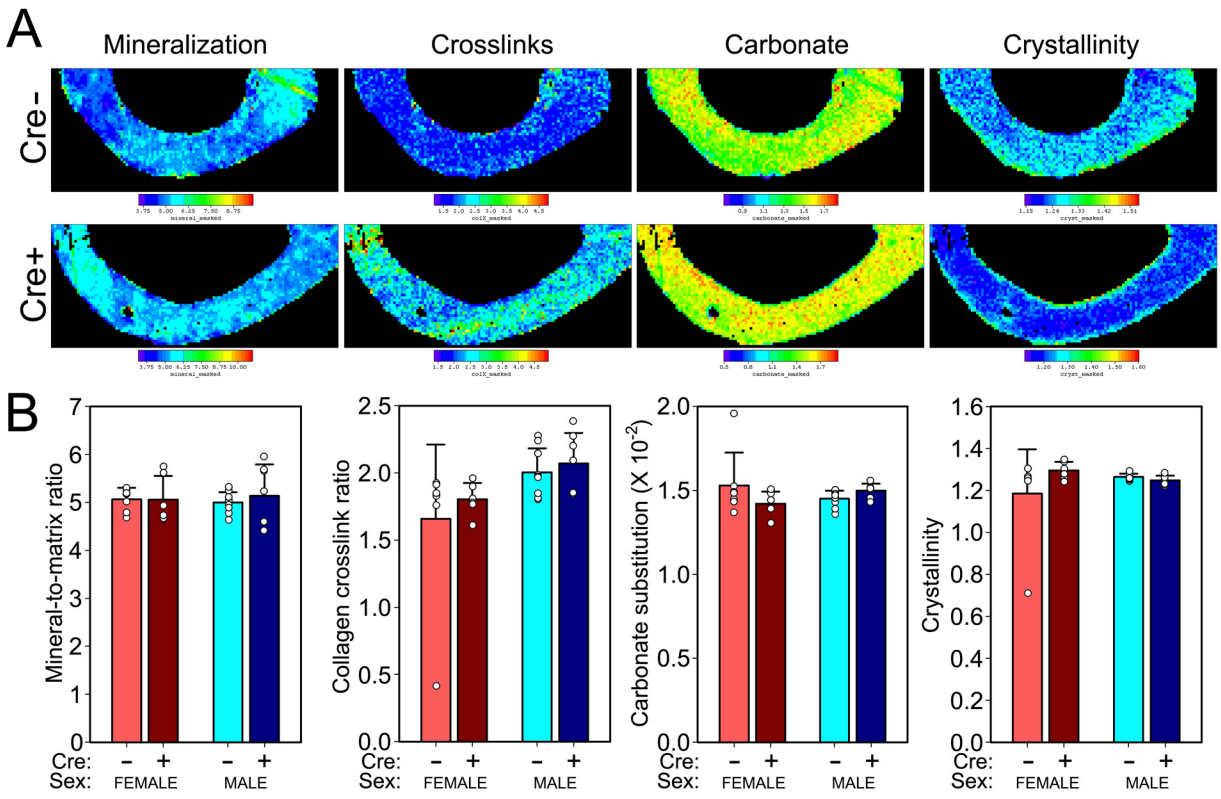

Figure S2: Cortical bone matrix composition measured at the humeral midshaft. Mineralization (mineral-to-matrix ratio), collagen crosslink ratio, carbonate substitution, and mineral crystallinity were measured from longitudinal cross-sections using Fourier transform infrared imaging (FTIRI) at the National Synchrotron Light Source at the Brookhaven National Laboratory. (A) Representative cross-sectional composition maps from female mice demonstrating the relative values for each parameter measured. Colormetric scale appears beneath each map. (B) Mineral-to-matrix ratio, collagen crosslink ratio, carbonate substitution, and mineral crystallinity by sex and ^{10kb}Dmp1-Cre status (all mice are Dkk1$^{f/f}$). All data panels were analyzed using unpaired t-tests within each sex (comparing Cre-positive to Cre-negative).

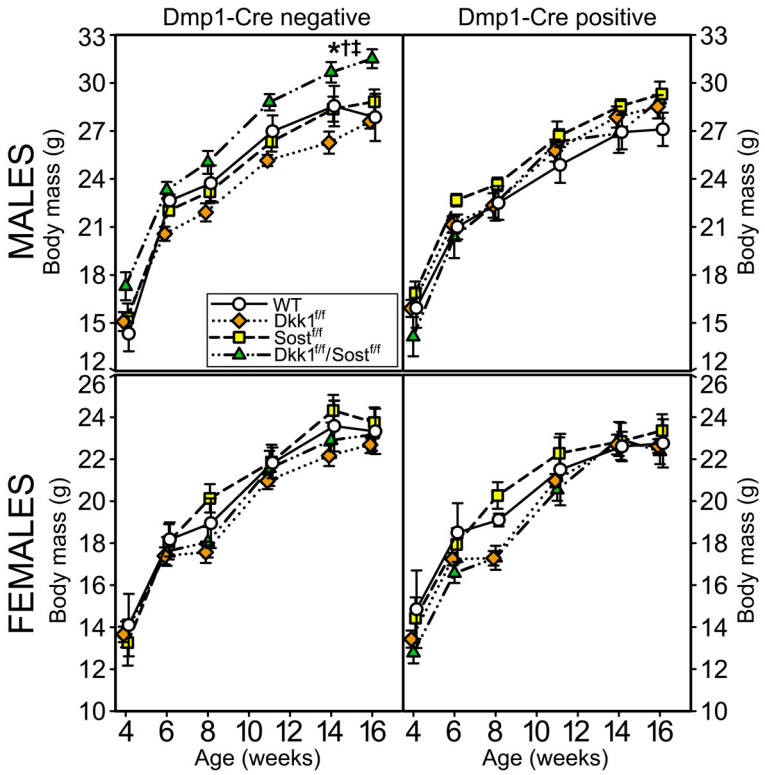

Figure S3: Body mass in WT (Dkk1$^{+/+}$; Sost$^{+/+}$), Dkk1-flox (Dkk1$^{f/f}$, Sost$^{+/+}$), Sost-flox (Dkk1$^{+/+}$; Sost$^{f/f}$), and compound flox (Dkk1$^{f/f}$; Sost$^{f/f}$) mice, collected every 2-3 wks. Panels to the left display data from Cre-negative mice, and panels to the right display data from Cre-positive mice. Upper panels are from male mice and lower panels are from female mice. *P<0.05 compared to WT mice. For all curves, N=6-14 mice/group. All panels were analyzed using repeated measures ANOVA followed by Fisher's protected LSD post hoc tests.

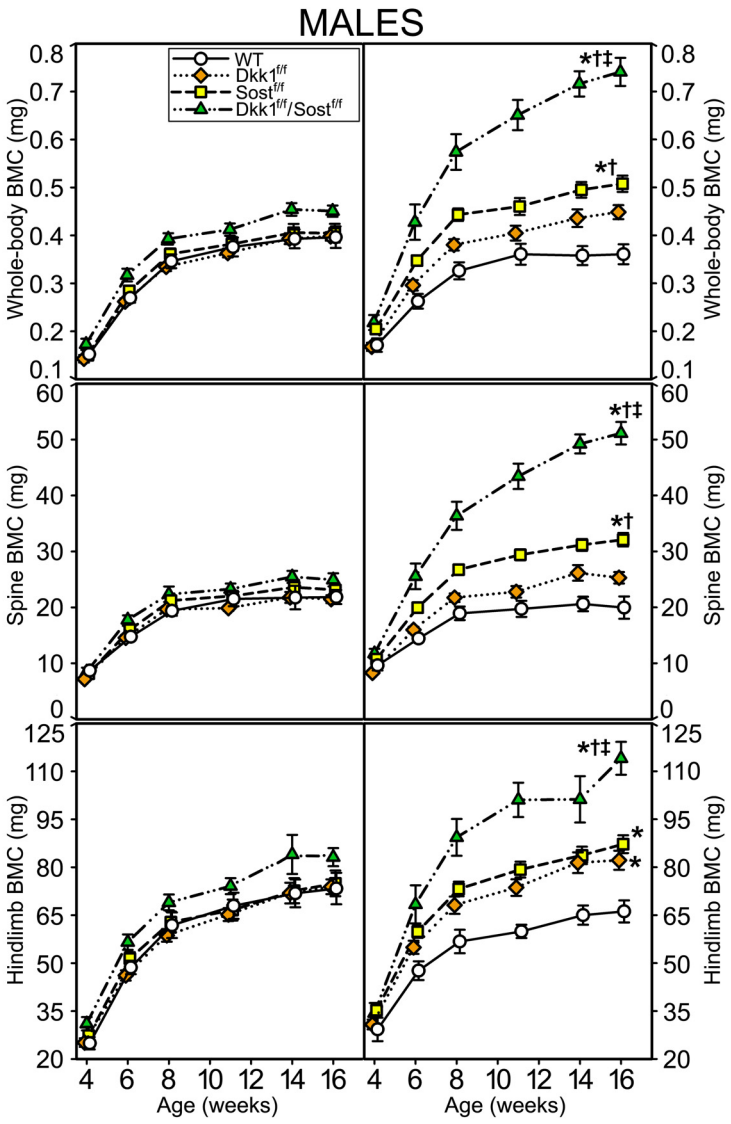

Figure S4: Serial in vivo DXA scans of WT (Dkk1$^{+/+}$; Sost$^{+/+}$), Dkk1-flox (Dkk1$^{f/f}$, Sost$^{+/+}$), Sost-flox (Dkk1$^{+/+}$; Sost$^{f/f}$), and compound flox (Dkk1$^{f/f}$; Sost$^{f/f}$) mice, collected every 2-3 wks and analyzed for (A & B) whole body BMC, (C & D) lumbar spine BMC, and (E & F) BMC of the right hindlimb distal to the acetabulum. Panels A, C, and E display data from Cre-negative mice only; panels B, D, and F display data from Cre-positive mice only. All panels are based on data on male mice; corresponding data from female mice are provided in Figure 3. *P<0.05 compared to WT mice; †P<0.05 compared to Dkk1f/f mice; ‡P<0.05 compared to Sostf/f mice. For all curves, N=5-12 mice/group. All panels were analyzed using repeated measures ANOVA followed by Fisher's protected LSD post hoc tests.

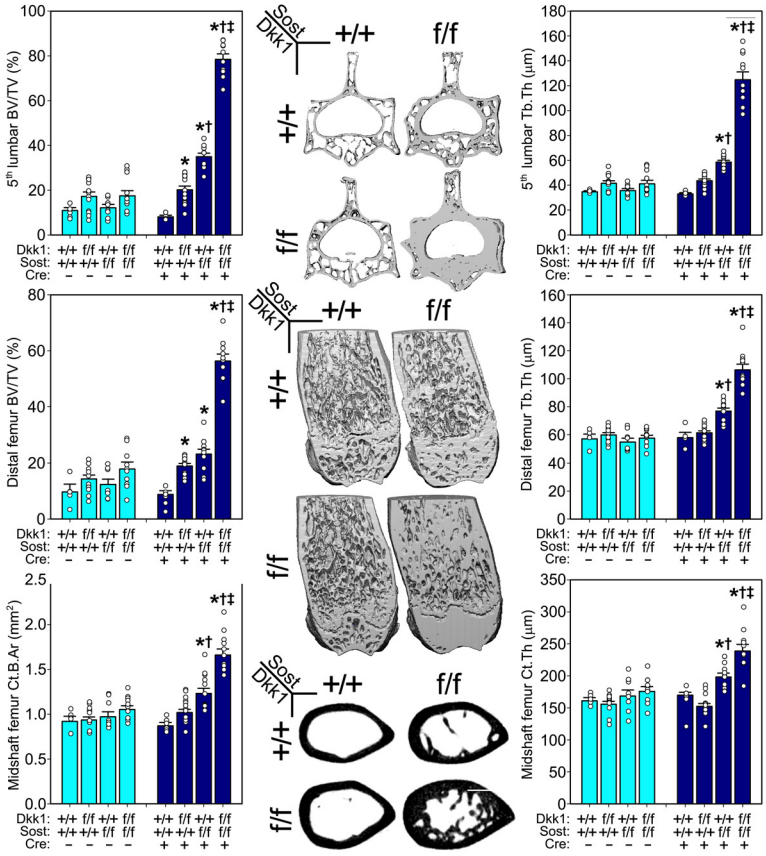

Figure S5: μCT-derived measurement of the 5th lumbar vertebral body cancellous bone, distal femur metaphyseal cancellous bone, and mid-femur cortical bone from WT (Dkk1$^{+/+}$; Sost$^{+/+}$), Dkk1-flox (Dkk1$^{f/f}$, Sost$^{+/+}$), Sost-flox (Dkk1$^{+/+}$; Sost$^{f/f}$), and compound flox (Dkk1$^{f/f}$; Sost$^{f/f}$) mice, with (dark blue bars) and without (light blue bars) the ^{10kb}Dmp1-Cre transgene. Quantitative differences in 5th lumbar trabecular bone volume fraction and thickness (BV/TV and Tb.Th; top row) can be appreciated from representative 3D tomographic reconstructions of the central 30% of the vertebra from Cre-positive mice. Quantitative differences in distal femur trabecular bone volume fraction and thickness (middle row) can be appreciated from representative 3D reconstructions of the caudal half of the distal femur (the ventral half was digitally removed) in Cre-positive mice. Quantitative differences in midshaft femur cortical bone area and thickness (Ct.B.Ar and Ct.Th, bottom row) can be appreciated from representative 2D slices taken from the femur mid-diaphysis of Cre-positive mice. All panels are based on data/images from male mice; corresponding data/images from male femice are provided in Figure 4. *P<0.05 compared to Cre-matched WT mice; †P<0.05 compared to Cre-matched Dkk1$^{f/f}$ mice; ‡P<0.05 compared to Cre-matched Sost$^{f/f}$ mice. For all panels, N=5-12 mice/group. All data panels were analyzed using 1-way ANOVA followed by Fisher's protected LSD post hoc tests.

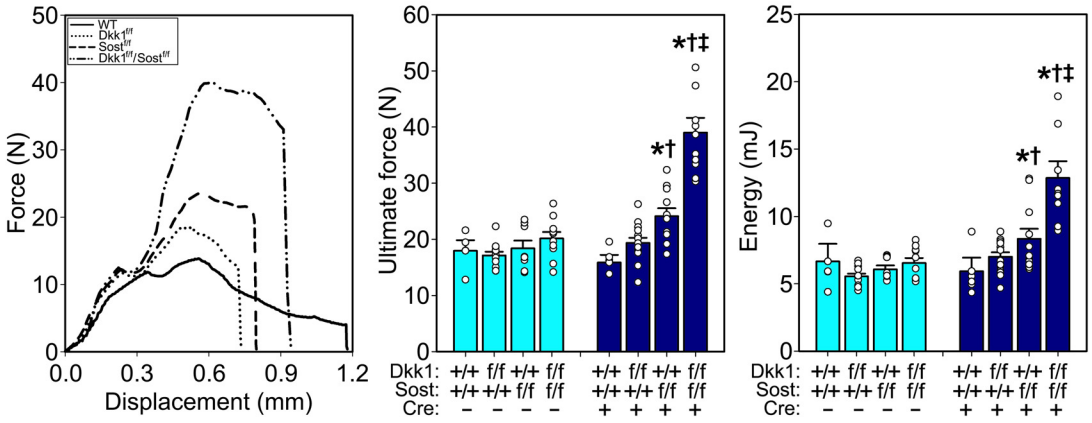

Figure S6: 3-point monotonic bending tests to failure conducted on whole femora from WT ($Dkk1^{+/+}$; $Sost^{+/+}$), Dkk1-flox ($Dkk1^{f/f}$, $Sost^{+/+}$), Sost-flox ($Dkk1^{+/+}$; $Sost^{f/f}$), and compound flox ($Dkk1^{f/f}$; $Sost^{f/f}$) mice, with (dark blue bars) and without (light blue bars) the 10kbDmp1-Cre transgene. (Left) Representative force–displacement curves from tests conducted on Cre-positive mice reveal differences in mechanical properties among genotypes; quantification of (middle) ultimate force (peak height of the curve) and (right) energy absorbed (area under the curve). All panels are based on data/images from male mice; corresponding data/images from female mice are provided in Figure 5. *P<0.05 compared to Cre-matched WT mice; †P<0.05 compared to Cre-matched $Dkk1^{f/f}$ mice; ‡P<0.05 compared to Cre-matched $Sost^{f/f}$ mice. N=7-13 mice/group. Data panels were analyzed using 1-way ANOVA within each Cre grouping, followed by Fisher's protected LSD post hoc tests.

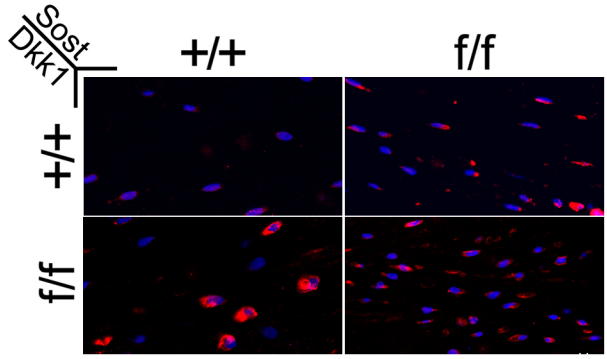

Figure S7: Immunohistochemical labeling of active β-catenin (non-phosphorlyated) in paraffin tissue sections from the tibial cortex of WT (Dkk1$^{+/+}$; Sost$^{+/+}$), Dkk1-flox (Dkk1$^{f/f}$, Sost$^{+/+}$), Sost-flox (Dkk1$^{+/+}$; Sost$^{f/f}$), and compound flox (Dkk1$^{f/f}$; Sost$^{f/f}$) mice. All mice are ^{10kb}Dmp1-Cre positive. Red staining indicates active β-catenin; blue staining (DAPI) indicates nuclei.

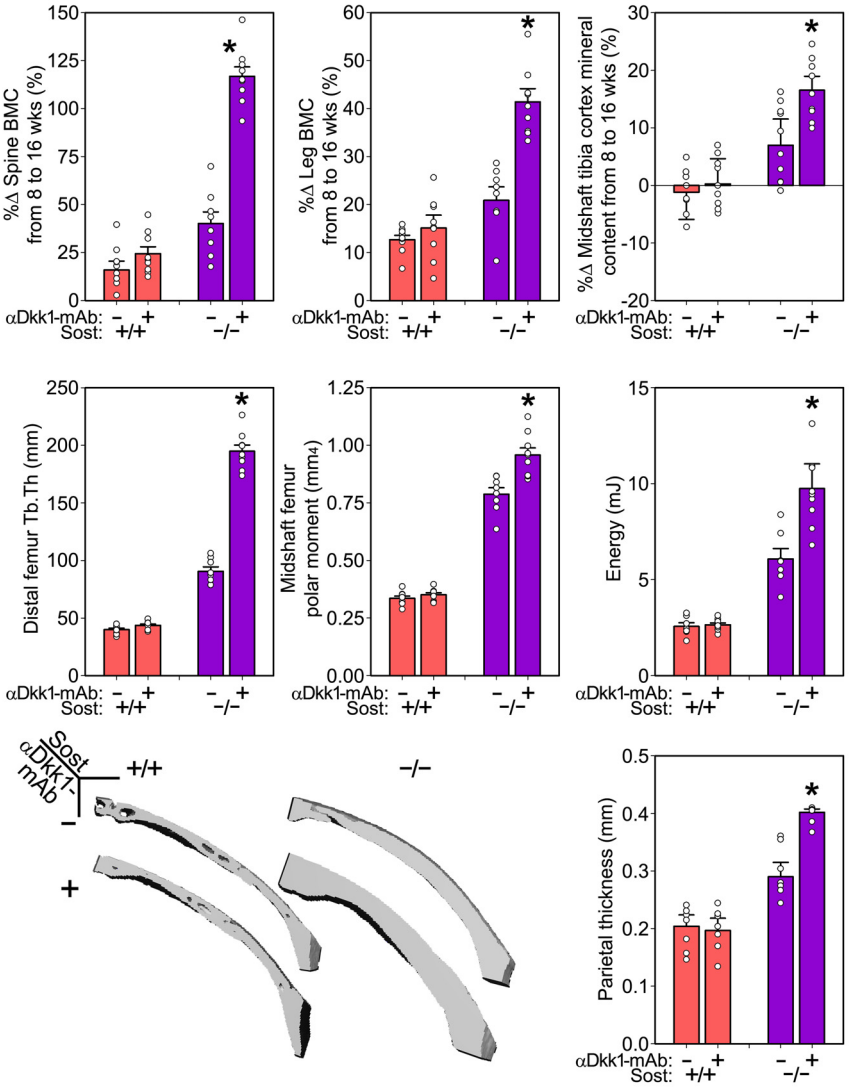

Figure S8: (Top row) Percent change in spinal bone mineral content (BMC) and leg BMC measured using DXA, and midshaft tibia BMC measured using pQCT, calculated from just prior to the start of treatment (at 8 wks of age) to sacrifice at 16 wks of age, capturing 8 wks of Dkk1 monoclonal antibody (αDkk1-mAb) or vehicle injection in WT (red bars) and Sost$^{-/-}$ (purple bars) mice. (Middle row) Femoral μCT-derived properties in the distal metaphyseal spongiosa (bone volume fraction; BV/TV) and midshaft cortex (polar moment of inertia), and energy to failure derived from 3-point monotonic bending tests to failure, measured in 16 wk-old mice, after 8 wks of vehicle or Dkk1 antibody treatment. (Bottom row) μCT-derived changes in parietal bone thickness in vehicle or Dkk1 antibody-treated WT and Sost$^{-/-}$ mice. All panels are based on data/images from female mice. *P<0.05 compared to genotype-matched vehicle-treated mice. For upper and middle panels, N=9-12 mice/group. For lower panel, N=6 mice/group. Data panels were analyzed using unpaired t-tests within each Sost background.

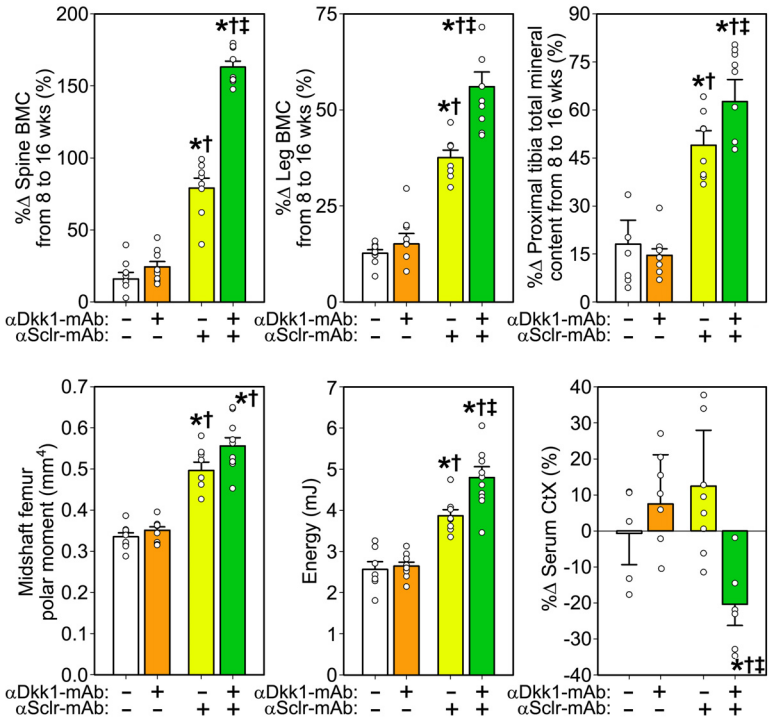

Figure S9: (Top row) Percent change in spinal bone mineral content (BMC) and leg BMC measured using DXA, and proximal tibia BMC measured using pQCT, calculated from just prior to the start of treatment (at 8 wks of age) to sacrifice at 16 wks of age, capturing 8 wks of Dkk1 monoclonal antibody (αDkk1-mAb, orange bars), sclerostin monoclonal antibody (αSclr-mAb, yellow bars) co-injection with both antibodies (green bars) or vehicle (solid bars) in WT female mice. (Bottom row) Femoral μCT-derived midshaft femur polar moment of inertia and energy to failure derived from 3-point monotonic bending tests in antibody- or vehicle-treated mice; and percent change in the bone resorption marker CtX, measured from serum samples taken just prior to the start of treatment (at 8 wks of age) and again 3 wks into the treatment regimen (11 wks of age). *P<0.05 compared to vehicle-treated mice; †P<0.05 compared αDkk1-mAb-treated mice; ‡P<0.05 compared to αSclr-mAb-treated mice. For upper panels, N=8-12 mice/group. For lower left and middle panels, N=10-11 mice/group. For lower right panel, N=6-8 mice/group. All panels were analyzed using 1-way ANOVA, followed by Fisher's protected LSD post hoc tests.